

# FTI Thermal Modelling using Rough Order Model

David Doyle,  
Curtiss-Wright, Aerospace Instrumentation Group,  
Unit 5 Richview Office Park, Clonskeagh, Dublin 14, D14 X981, Ireland  
ddoyle@curtisswright.com

## Abstract

There is an industry drive in Flight Test Instrumentation to make the acquisition units smaller and more powerful; smaller with less weight to fit in tighter, more disturbed locations; and more powerful to facilitate fast, powerful, high-speed chips and to provide excitation to sensors.

This drive to minimization and high-power means that thought needs to be given to thermodynamics and the management of heat dissipation. This in turn means that tools and Techniques to predict thermal performance are becoming more and more important.

This paper is a study of a thermal modelling technique using a rough order model and open source pSpice to run the thermal system as an analogous electronic circuit. With this tool we can predict the thermal performance the installation with a view to having a successful flight test campaign.”

**Key words:** Thermal Modelling, Rough Order Model (ROM)

## Introduction

Modelling temperature in a complex electronic system like flight test instrumentation is a very complex and difficult task. There are hundreds of passive and active components on each board each with their own heat dissipation requirements and thermal properties. They all make a very complex thermodynamic system. To be practical, there needs to be an approximation that simplifies the process of modelling the thermodynamic behavior. This is especially true for a modular system where units can be assembled in any combination. The approximation used in this study is a rough order thermal model. This operates with fundamental thermodynamic principles operating on conceptual approximations of the physical units under study.

## Rough Order Model

At the center of the rough order model is a node of specific dimensions. This node is assigned thermodynamic properties and is considered to have a heat flow through it as per Fig 1.

In particular, the rate of heat flow is directly proportional to the temperature differential on either side of the node, the cross-sectional area of the heat flow and a constant call the thermal conductivity which is a property of the material.

The rate of heat flow is inversely proportional to the distance across the node in the direction of the heat flow.

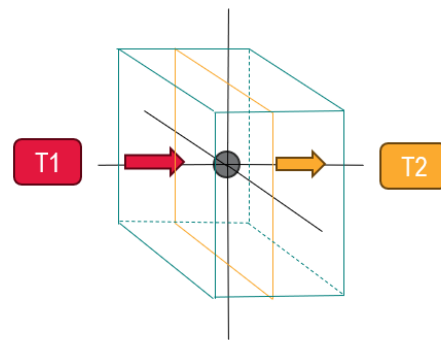


Fig. 1. Representation of a rough order node

$$Q = k A \frac{(T_1 - T_2)}{X_{12}}$$

**Q** rate of heat flow (W)  
 Temperature T1 and T2 (K)  
**X<sub>12</sub>** Distance between 1 & 2 (m)  
**A** cross section area (m<sup>2</sup>)  
**k** Thermal conductivity of medium (W/Km)

Fig. 2. The fundamental thermodynamic equation that governs the ROM node.

The heat flow equation has the same form as like ohms law in Fig 3. This means that we can use freely available electronic circuit simulators to handle the numerical analysis, provided suitable numbers are provided to the model.

$$I = \frac{V1 - V2}{R}$$

I Current flow in (A)  
 V1 – V2 Voltage Differential (V)  
 R Electrical Resistance ( $\Omega$ )

Fig 3. Ohms Law

The nodes are generally smaller than the material being modelled and can be combined into a mesh as per figure 3. This allows for a predicted temperature along medium. In the case where there is a break in the medium and a boundary to another, this boundary can be modelled as an extra thermal resistance.

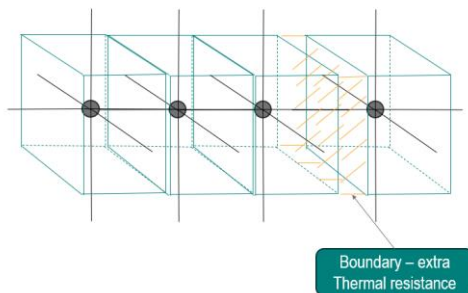


Fig. 4. Mesh of ROM nodes with a boundary condition.

For the purposes of using an electrical circuit simulator to simulate thermal behavior the thermal/electrical equivalents in Fig 5 were used.

Thermal Capacitance (J/K)  $\approx$  Electrical Capacitance (F)  
 Thermal Resistance (K/W)  $\approx$  Electrical Resistance ( $\Omega$ )  
 Power Dissipation (W)  $\approx$  Constant Current Source (A)  
 Temperature (T)  $\approx$  Voltage (V)  
 Ambient Temperature (K)  $\approx$  Electrical Ground (0V)

Fig. 5. Thermal/Electrical equivalent used in this study

Considering the above, a circuit can be used to predict the thermal system's dynamic and steady state, that is given the thermal properties of the materials involved, the correct boundary conditions and the correct wattages of the heat sources.

Fig 6 shows the 3D image of a data acquisition unit side by side with its equivalent electrical circuit that represents its thermal behaviour. The ROM model is an approximation and that

each PCB is modelled as a single node and a single block. It does not model each of the components placed on the PCB.

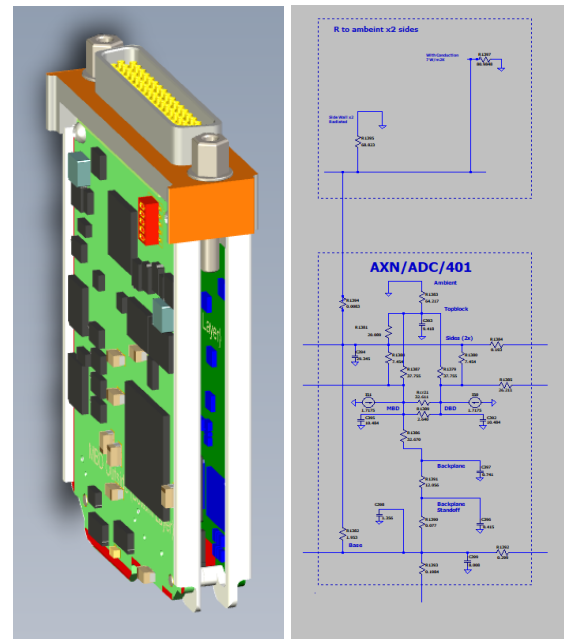


Fig. 6. Representative of physical data acquisition and its equivalent thermal circuit.

The circuit in Fig 6 represents a dual board user module in the data acquisition system. With a library of circuits representing all the available user modules any combination of user modules can easily be assembled into a thermal system representing the physical system.

Finally, to do a thermal simulation the following elements are needed:

1. The system configuration of the planned instrumentation
2. A power calculator tool to establish the power dissipation requirements per board.
3. A library of equivalent thermal circuits that represent user modules and chassis.
4. A thermal model of the physical bracket that the equipment is mounted on if it needs to be modelled (if it can be heated by the equipment)

**Procedure**

The system in Fig 7 was modelled with the ROM Thermal Model and assembled in reality to compare the thermal model with the experimentation. The system was set up on an AXN/CHS/16U/AB2 which permitted the deployment of heat sinks AXN/HSK/16U/V. The experiment ran the with and without the heat sinks fitted. The unit was not mounted to any plate or bracket during test.

Slot #	Module Selection
Chassis	AXN/CHS/16U/AB1
0	AXN/BCU/402/C
1	AXN/ADC/401
2	AXN/ADC/401
3	AXN/ADC/401
4	AXN/ADC/401
5	AXN/ADC/401
6	AXN/ADC/401
7	AXN/ADC/405/10V
8	AXN/ADC/405/10V
9	AXN/ADC/404/B
10	AXN/ADC/404/B
11	AXN/ADC/404/B
12	AXN/ADC/404/B
13	AXN/MBM/401
14	AXN/MBM/401
15	SPARE
16	SPARE

Fig. 7. User module loadout of the AXN/CHS16U/AB2 test article for the experiment

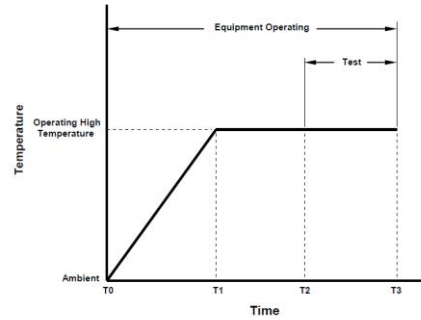
The 6x AXN/ADC/401 are each 8x channel bridge cards and all 48x channels had a 15mA excitation load arranged for the test.

The 4x AXN/ADC/404/B are each 12x channel bridge cards and all 48x of those channels had a 15mA load arranged for the test.

The 2x AXN/ADC/405/10V are each 24x channel differential ended voltage cards. These had a precision voltage applied to all 48 channels.

The 2x AXN/MBM/401 are each 4x Dual redundant MIL-STD-1553 bus monitor cards. One of them had all 4x channels connected to a MIL-STD-1553 simulator.

The test method chosen was the DO160-G Category D2 hot test ( 70C )



- Note: 1) Temperature change rate from T0 to T1 is not specified.
- 2) T1 to T2 is time for equipment temperature to stabilize.
- 3) T2 to T3 is 2.0 hours, minimum.

Figure 4-4 Operating High Temperature Test

Fig. 8. Temperature profile for DO160-G Category D2 high operating thermal test

The block diagram for the test system is as per Fig 9. and photos of the test article are in Fig 10

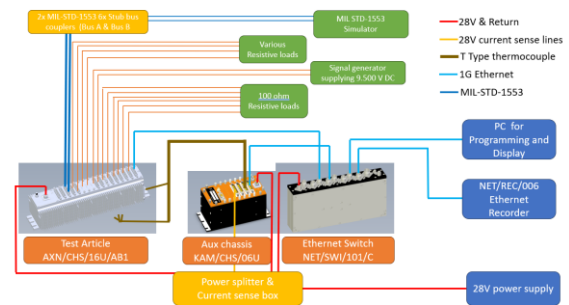


Fig. 9. Temperature profile for DO160-G Category D2 high operating thermal test



Fig. 10. AXN/CHS/16U/AB2 test article in thermal chamber with thermcouple.

In parallel with the experiment, the ROM for each scenario was developed in LTSpice which is an open source circuit simulator package. (Fig 11 and Fig 12)

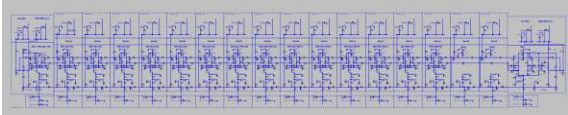


Fig. 11. Equivalent thermal circuit of AXN/CHS/16U/AB2 test article without heat AXN/HSK/16U/V heatsinks

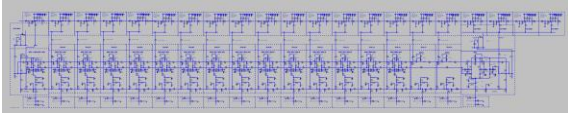


Fig. 12. Equivalent thermal circuit of AXN/CHS/16U/AB2 test article without heat AXN/HSK/16U/V heatsinks

These simulations were run to compare the simulation results with the indicated values in the experiment.

To run the model certain assumptions were made related to heat transfer boundary conditions and power distribution as follows in Fig 13

Air convection with an equivalent Conductance of  $26 \text{ W/m}^2\text{K}$

Emissivity  $\epsilon$  of 0.9 for Axon Chassis for radiation purposes (black body)

Emissivity  $\epsilon$  0.16 for exposed based plate

Thermal Interface material between AXN/HSK/16U and chassis with  $7.0 \text{ W/mK}$

The potential path to conduct heat away from the DAU through the sensor wiring will not be modelled (and will not cool down the DAU in the simulation)

The potential path to conduct heat through the grill in the oven will not be modelled

Power consumed by user modules as described in the datasheets equally split between mother board and daughter board in dual board user modules

Power consumed externally by sensor excitations do not heat up the test article

Fig. 13. Assumptions used in ROM model

## Results

There are two significant measured results, the measured power consumption and the measured temperature at different points on the test article. Two separate experiments were run, one with the AXN/CHS/16U/AB2 test article with AXN/HSK/16U/V heatsinks fitted and the other without the heatsinks fitted.

The power consumption was measured at two points, at the external power supply and inside the test article. The current was measured on the 28V line so power consumption could be calculated. This was compared with the predicted power consumption from the user module datasheet specifications and from the prediction of the Axon power supply unit's losses based on predicted efficiency at the predicted load. The second point where current was measured was on the Axon 15V backplane supply. The results of both are shown in Fig.14

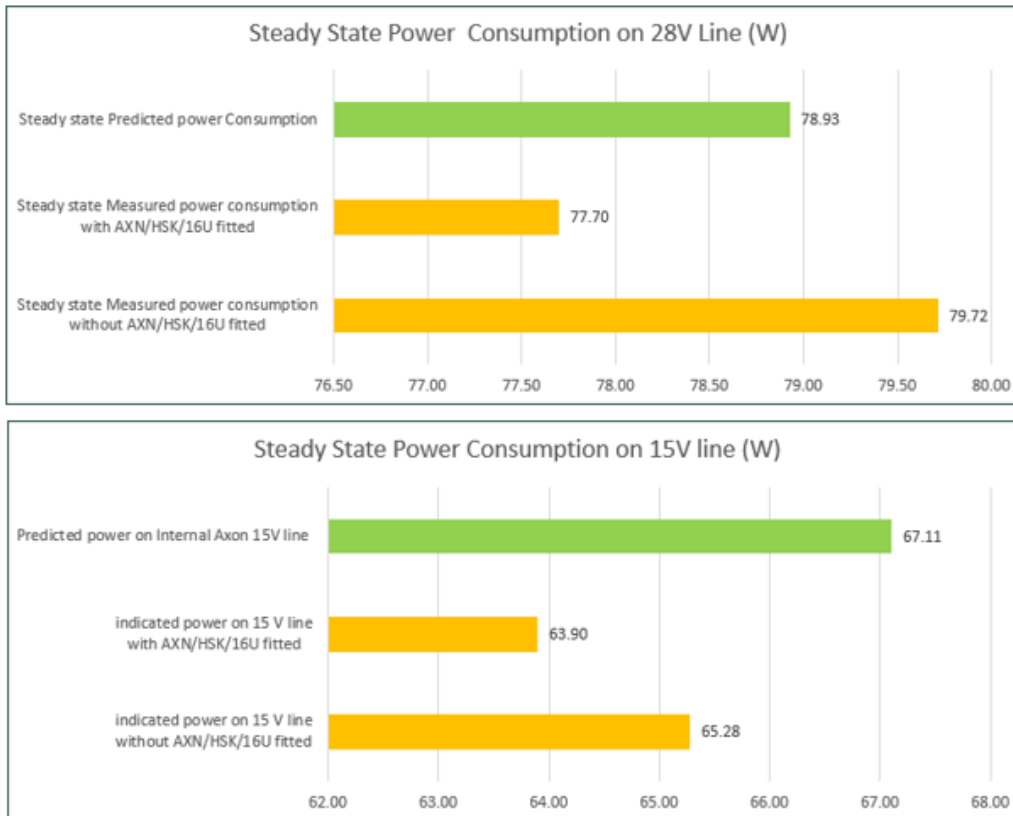
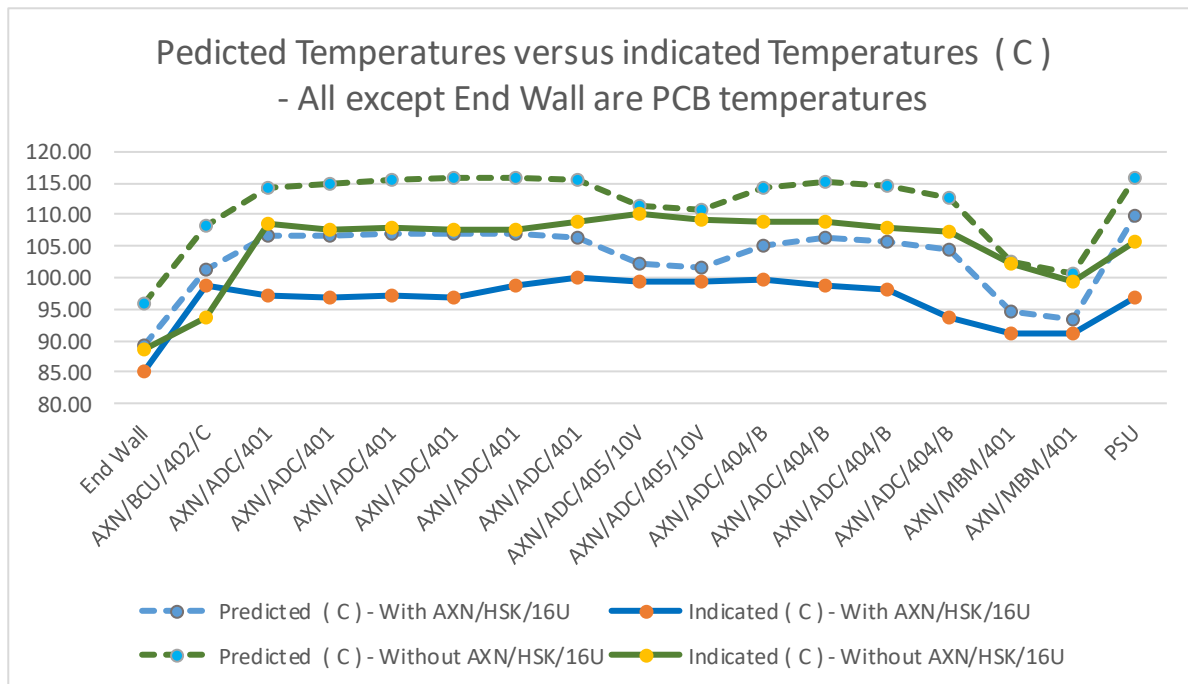


Fig. 14. Predicted and measured power consumption

In each case the measured power consumption with the heatsinks fitted was less than the measured power consumption with the heatsink. The measured power consumption on the 28V line with a heatsink fitted was 2.45% less than predicted, without the heatsink the power consumption was 1% more than predicted. In both cases the expected power consumption figure on the Axon backplane was less than predicted. With the heatsink fitted it was 4.78% less than predicted and without the heatsinks fitted

The indicated temperature points were read directly from the board of the user modules with the inbuilt Axon resistance temperature device. In addition to that the end wall of the AXN/CHS/16U/AB2 had an R-Type thermocouple mounted on it to measure the case temperature. The results from both tests are as shown in figure 15



In both cases, the measured temperatures were below the predicted temperatures.

*Fig.15.Predicted Temperatures vs indicated temperatures.*

## Conclusions

The rough order thermal model was proven to be conservative. This is due to the inbuilt headroom of the model and the assumptions made. This makes it a good tool in terms of risk reduction for flight test instrumentation programs.

The technique has proven to be useful for modular flight test instrumentation systems. The downside of this technique is when the thermal study requires a complex bracket because this can be time consuming to generate.

In practice, the model has been used to assist with the design of the mounting brackets on flight test instrumentation deployment, it has been used to guide thermal risk reduction steps on flight test instrumentation deployments and it has been used to guide product development decisions. In this way the technique has proven its worth.

Further research for this topic is to compare the predicted temperatures with the indicated temperature for the actual flight tests of the flight test instrumentation studies that were made with the model.

## The main Acknowledgements

The main body of work that this study is built on the work by Professor Jeff Punch, School of Engineering University of Limerick, Ireland. Jeff specialises in thermal sciences and did extensive work modelling for the Curtiss Wright space team in Dublin Ireland.

## References

- [1] RTCA, Incorporated, DO-160G, Environmental Conditions and Test Procedures for Airborne Equipment; doi December 8, 2010.
- [2] Curtiss-Wright, DST/AJ/011, AXN/CHS/16U/AB2; doi 20 Nov. 2023
- [3] Curtiss-Wright, DST/AH/004, AXN/BCU/402/C; doi 21 Apr. 2023
- [4] Curtiss-Wright, DST/AB/019, AXN/ADC/401; doi 19 Jul. 2023
- [5] Curtiss-Wright, DST/AB/019, AXN/ADC/404/B; doi 23 Jan. 2023
- [6] Curtiss-Wright, DST/AB/019, AXN/ADC/405/10V; doi 23 Jan. 2023
- [7] Curtiss-Wright, DST/AF/002, AXN/MBM/401; doi 16 Apr. 2024